SAND2000-1209J

J. Phys. D: Appl. Phys. 33 (2000) 1–7. Printed in the UK

PII: S0022-3727(00)08429-1

Role of beam absorption in plasma during laser welding

V V Semak†||, R J Steele‡, P W Fuerschbach§ and B K Damkroger§

† Physics Department, New Mexico State University, Las Cruces, NM 88003, USA
‡ Naval Air Warfare Center, China Lake, CA 93555-6100, USA
§ Sandia National Laboratories, Albuquerque, NM 87185-0367, USA

Sunrise Setting
Marked Proof
D/108429/PAP
19152ae
Printed on 27/3/00
at 12.32

Received 4 October 1999

Abstract. The relationship between beam focus position and penetration depth in CW laser welding was studied numerically and experimentally for different welding conditions. Calculations were performed using a transient hydrodynamic model that incorporates the effect of evaporation recoil pressure and the associated melt expulsion. The simulation results are compared with measurements made on a series of test welds obtained using a 1650 W CO_2 laser. The simulations predict, and the experiments confirm, that maximum penetration occurs with a specific location of the beam focus, with respect to the original sample surface, and that this relationship depends on the processing conditions. In particular, beam absorption in the plasma has a significant effect on the relationship between penetration and focus position. When the process parameters result in strong beam absorption in the keyhole plasma, the maximum penetration will occur when the laser focus is at or above the sample surface. In a case of weak absorption however, the penetration depth reaches its maximum value when the beam focus is located below the sample surface. In all cases, the numerical results are in good agreement with the experimental measurements.

1. Introduction

High-energy-density welding processes, such as laser and electron beam, provide an opportunity to obtain relatively narrow and deep welds. This property makes these processes advantageous in applications when the highest possible aspect ratio (ratio of weld depth to width) is required. Frequently, beam welding is applied when fine control over the penetration depth must be achieved. An example of such application is welding of a 'sandwich' structure, when the top layers must be joined and the bottom layers remain intact. Thus, issues of obtaining the highest possible penetration depth and control over the depth of welding gain larger practical importance as beam welding technology moves into the area of high-tech processing, which requires fine tuning of the process.

The control over the penetration depth can be achieved by varying the laser power, beam intensity distribution (beam mode composition, focusing system parameters, etc), position of the focal point relative to the sample surface, sample translation speed, and shield flow parameters such as shield gas chemical composition, flow geometry, mass rate, etc. Also, the keyhole plasma, whose parameters are defined by the chemical composition of the sample and vapour gas dynamics in the keyhole, can have a strong influence on the penetration depth. This, perhaps, incomplete list includes enough parameters to make the matrix of experimental studies quite large and a pure empirical approach impractical. Obviously, the solution could be found in the creation of a model which is capable of providing the predictive process control and to limit the experimental work by the verification runs.

There are currently two types of model that address the issue of prediction of welding depth for the different processing parameters. Typical examples of the model of the first type can be found in the references [1–4]. These models, developed on the basis of an analytical approach and proposed by Rosenthal more than 50 years ago [5], describe a stationary temperature field, which is induced in a work-piece by a moving line or point heat source. The works [1–4] introduced a modification in Rosenthal's model which was not concerned with the nature of the heat source. This modification consisted in representing a line heat source by a vapour–plasma filled channel, called a keyhole. In this modified approach the main problem is determining the strength of a line heat source. If the line heat source strength is found, then for the given laser beam power and beam translation speed the value of welding penetration can be computed. Typically the source strength is calculated either assuming that all laser radiation is absorbed in the keyhole plasma and then is transferred to the keyhole wall [3], or considering the direct absorption of the laser radiation at the keyhole wall [4]. The detailed critique of the models of first type is not a goal of this article. However, several major errors of the described approach have to be mentioned.

|| Currently address: ARL, Pennsylvania State University State College, PA 16804, USA.

First, the majority of the models similar to those described in the [1–4] assume that the surface of the keyhole is at the boiling temperature. Thus, after determining the heat source strength, the temperature field is computed using the standard heat conduction equation in a moving media with a fixed temperature on the surface of the heat source as one of the boundary conditions. Detailed analysis of the welding models of the first type shows that the authors of these works have provided neither theoretical nor experimental support for the assumption of the keyhole surface being at the boiling temperature. On the contrary, there are theoretical works which do not use this assumption [6, 7]. These works display logically consistent results; the melt surface temperature depends on the value of absorbed laser intensity and, therefore, can be lower than, equal to, or higher than the boiling temperature. It is worth mentioning that the melt surface temperature can exceed the boiling temperature because laser interaction under typical conditions is accompanied by only surface evaporation, and volumetric evaporation, called boiling, does not occur [8].

Secondly, in the models of the first type the calculations of the intensity of the laser beam absorbed on the keyhole wall in the presence of multiple reflections is performed under assumption of conical or other simple axisymmetric stationary shape of the keyhole. Such an approach can lead to a significant error. Indeed, when the keyhole depth increases the angle of incidence becomes large. For a majority of metals the absorption coefficient varies significantly when the angle between the beam axis and normal to the surface exceeds 60–70°. Consequently, the distribution of the absorbed intensity ought to be strongly dependent on the keyhole shape. Therefore, the calculation of the source strength must be performed using a self-consistent approach, which takes into account the change of the keyhole shape depending on the distribution of absorbed intensity and calculates a new intensity distribution for the changed keyhole. None of the current models of the first type incorporate such self-consistent keyhole shape–absorbed intensity calculations.

However, even if the above described drawbacks would be corrected, the models, such as in [1–4], still cannot be used for the adequate simulation of keyhole laser welding under typical industrial conditions. The reason for that is due to a steady-state keyhole postulation which is the core assumption of the models of the first type. Thus the main feature of the models [1–4] is that they are steady-state models. This means that the keyhole is assumed to develop (reach maximum possible depth) during a time much smaller than the typical interaction time given by either the pulse duration or the ratio of the beam diameter and the beam translation speed. In other words, it is supposed that the keyhole develops instantly relative to the other characteristic times. After the steady state is reached it is assumed that the balance of evaporation recoil pressure and sum of surface tension and hydrostatic pressures exists on the keyhole wall. However, measurements of the dynamics of laser beam penetration in the metal samples show that the time required for a keyhole to reach a steady depth lies in the range of 20–50 ms [9, 10]. This is a large time compared to the characteristic times of the process. Thus, under the typical industrial processing conditions the keyhole is essentially non-stationery and remains in the state of growth throughout the interaction time. Consequently, the balance of pressures on the wall does not exist. On the contrary, the evaporation recoil pressure dominates resulting in a drilling-like propagation of the keyhole into material. The steady keyhole models could be adequate for a very slow (less than 1 mm s^{-1}) welding speed or a very long (greater than 100 ms) pulse duration. However, the latter assumption also needs verification.

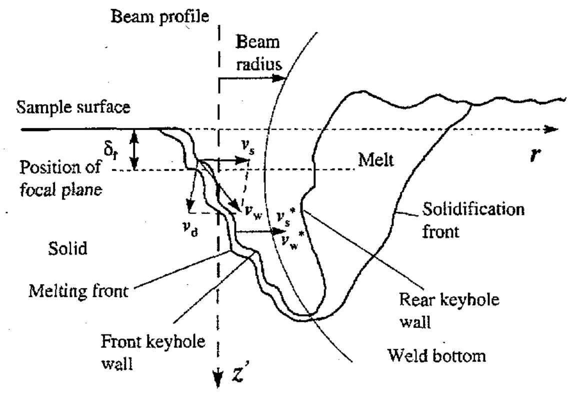

Figure 1. Schematic diagram of the physical model for non-stationary laser keyhole welding.

The laser welding models of the second type are based on a non-stationary keyhole approach. Only recently the concept for a transient keyhole model was proposed, independently, by the physicists in the US and France [10, 11]. The number of publications related to the laser welding simulation using the non-stationary approach is still small [10–13] and the transient keyhole welding model is still under development. However, the numerical codes created on the basis of the transient keyhole model can already be used for semi-quantitative simulation of high-energy-density welding. This article illustrates the capability of the proposed transient keyhole model to simulate the welding penetration depth as a function of laser power, beam translation speed, and relative position of the beam focal plane. In particular, the extreme importance of the absorption of a laser beam in the keyhole plasma is demonstrated.

2. Model

A transient model for the front keyhole wall and the corresponding numerical code were developed recently [14]. This model allows calculation of welding front dynamics from the first principals. The approach for simulation of penetration depth is schematically shown in figure 1. According to the transient keyhole model [11], the front part of the keyhole is exposed to the laser beam. The back part of the keyhole wall is kept outside the laser beam due to the pressure of the vapour jet in the keyhole. The evaporation from the surface of the melt on the front keyhole wall results in the generation of the recoil pressure. This excessive pressure produces melt ejection in the sidewise direction, and both the melt surface and the melting front propagate forward similarly to laser drilling [12, 13]. The

DISCLAIMER

DISCLAIMER

velocity of the front propagation is determined by melt ejection and melt evaporation [13], which depend on the melt surface temperature and, consequently, on the absorbed beam intensity. A value of local velocity of the keyhole wall, v_d, can be calculated knowing the local absorbed intensity, beam radius, and material properties and using an approach described in the [13]. The vector of local keyhole wall velocity is normal to the wall surface. Thus, calculating the value of the local keyhole wall velocity, directing the vector v_d normally to the keyhole wall, and adding the vector velocity of the sample translation in the beam coordinate system, v_s, one can obtain the vector of 'phase' velocity of the keyhole wall in the beam coordinate system, v_w (figure 1). We use the term 'phase' velocity because this is motion of the liquid–vapour interface, which does not represent mass motion. Computing the velocity v_w at all locations of the keyhole wall, one can determine the time-dependent shape of the front keyhole wall and, correspondingly, the depth of welding.

The calculation of the local velocity of the keyhole wall, v_d, can be performed if the value of laser intensity at the keyhole wall is known. The value of beam intensity at the keyhole wall can be calculated if the spatial distribution of plasma absorption coefficient is available. Unfortunately, measurements of the plasma absorption coefficient are practically impossible due to the restricted access to the volume inside the keyhole. The plasma absorption coefficient can be calculated. This calculation requires simulation of the evaporation from the front part of the keyhole and the gas dynamics of the vapour inside the keyhole. The model presented in [14] provides data on the evaporation rate and vapour temperature at the exit from the Knudsen layer. These results can be used as input parameters for a model, which calculates the density and temperature distributions in the vapour flow, distribution of electron density, and related absorption coefficient of plasma. Such a model must be self-consistent. That is, the temperature of vapour flow is calculated with the account of laser power absorbed in plasma, and the absorption coefficient of plasma is determined from the local vapour density and temperature. To the knowledge of the authors such a self-consistent simulation of a keyhole plasma has not yet been reported. The development of the outlined plasma model, which will incorporate transient model of the front keyhole, vapour gas dynamics in the variable shape keyhole, vapour ionization, and plasma heating due to laser beam absorption is in progress.

Additionally to the detail simulation approach, the effect of plasma in laser welding can be studied by comparison of the experimental data with the calculation results obtained by the model presented in [14] assuming a synthetic distributions of the plasma absorption coefficient.

To study the effect of plasma absorption on welding depth we use a simplified approach similar to that proposed by Fabbro [10] instead of our detail front keyhole model [14]. This approach allowed faster, although less exact, calculations. The rational and description for this simplified approach are given below.

The keyhole velocity is determined by the value of absorbed intensity and, generally, does not equal the beam translation velocity [12]. For a given beam intensity distribution there might exist a range in which the beam translation speed is lower than the component of keyhole wall velocity parallel to the sample surface. In this case the keyhole wall moves forward faster than the beam, which results in so-called 'runaway instability' [12, 14] accompanied by the generation of humps on the front keyhole wall surface, as shown in figure 1. The humps originate at the keyhole top and move downward along the wall surface. The normal to the keyhole wall surface in the hump area is closer to the beam axis. Therefore, the direction of the drilling velocity v_d can be approximately assumed as parallel to the beam axis (figure 1). This allows easy computing of the resulting front velocity v_w. The inclination of the wall between the humps is so steep and the angle of the beam incidence is so high that the absorbed intensity is not high enough to produce noticeable drilling [12]. Thus between the humps the drilling velocity v_d is practically zero and the front velocity there coincides with the sample velocity v_s (figure 1).

The dependence of drilling velocity, v_d (I_{abs}, r_l), on absorbed beam intensity, I_{abs}, and beam radius, r_l, was recently numerically computed [13] for the case of established flow (steady-state) condition. Due to the complicated dependence of the melt ejection and evaporation on the absorbed intensity and the beam radius, the function $v_d(I_{abs}, r_l)$ can not be expressed analytically. However, for the sake of convenience the numerically-determined dependence [13] can be approximated in the range of absorbed intensities less than 5 MW cm^{-2} as the following function:

$$v_d = k(I_{abs} - I_{th})^{1/2} \qquad (1)$$

where k is the proportionality coefficient and I_{th} is the threshold intensity at which the drilling disappears and the keyhole wall (or liquid–vapour interface) cannot propagate into the material bulk. From the numerical results presented in the [13] the approximate value of the proportionality coefficient in equation (1) can be estimated as $k \sim 510^{-6}$ (m s^{-1}) (W m^{-2})$^{1/2}$. The intensity absorbed on the surface of a hump which has the coordinates $(r, z = h)$ is

$$I_{abs}(r, z) = AI(r, z) \exp\left(-\int_0^{h(r)} \mu(z)\, \mathrm{d}z\right) \qquad (2)$$

where A is the surface absorptivity for a zero angle of incidence (we assumed that the hump surface is approximately perpendicular to the beam axis), $I(r, z)$ is the local intensity in the laser beam, and $\mu(z)$ is the absorption coefficient in the keyhole plasma. The expression for the absorbed intensity, (2), is written assuming that the multiple reflections provide a negligibly small addition to the directly absorbed beam. In order to determine the validity of this assumption, the simulation of beam propagation in the complex keyhole cavity is required. However, at the moment the model predicting shape of only the front part of the keyhole [14] is available. Known attempts assuming conical shape of the keyhole, such as in [4], cannot be correct due to the sharp angular dependence of the surface absorptvity.

We assume that the radial intensity distribution in any location of the laser beam is Gaussian, thus,

$$I(r,z) = I_0(z)\exp\left(-\frac{2r^2}{r_1^2(z)}\right) = \frac{2P}{\pi r_1^2(z)}\exp\left(-\frac{2r^2}{r_1^2(z)}\right) \quad (3)$$

where $I_0(z)$ is the beam intensity at the axis, P is the laser beam power, and $r_l(z)$ is the laser beam radius at the $1/e^2$ intensity level. The variation of the radius of an imperfect Gaussian beam with the coordinate z is given by the formula used in [15] and modified to represent a beam radius variation in the coordinate system related to the sample surface

$$r_1(z) = r_0\left[1 + \left(M^2\frac{\lambda(z+\delta_f)}{\pi r_0^2}\right)^2\right]^{1/2} \quad (4)$$

Here r_0 is the beam radius in the focal plane, M^2 is the beam quality parameter, λ is the laser wavelength, and δ_f is the position of the focal plane relative to the sample surface (δ_f is negative if the focal plane is below the sample surface located at $z = 0$).

To generate the synthetic distribution of the plasma absorption coefficient we accepted several simplifying assumptions which, perhaps, do not affect the generality of the data obtained. First, the spatial distribution of the plasma absorption coefficient is assumed to depend only on the z-coordinate and to be independent of radius. Second, because the plasma absorption strongly depends on both vapour gas dynamics and the laser beam intensity distribution it is logical to assume that the axial distribution of the absorption coefficient $\mu(z)$ has a maximum located at some distance below the focal plane. For the demonstration calculations we used the following distribution of laser radiation absorption coefficient:

$$\mu(z) = \mu_0\left(1 + \left(M^2\frac{\lambda(z+\delta_f-\Delta)}{\pi r_0^2}\right)^2\right)^{-\alpha} \quad (5)$$

where μ_0 is the maximum absorption coefficient of plasma, Δ is the distance from the focal plane to the cross section where plasma absorption coefficient is maximum, and α is the empirical parameter. The function $\mu(z)$, given in form of equation (5), corresponds to the dependence $\mu(z) \sim 1/(r_l^2)^\alpha$ with coefficient of proportionality μ_0 and shifted by distance Δ relative to the focal plane inside the sample (positive z-axis direction). This dependence reflects the assumption about the qualitative behaviour of the plasma absorption coefficient, which is assumed to be determined by vapour gas dynamics and beam intensity, and, therefore, must be proportional to some power of the local beam cross section. Numerical calculations show that the best coincidence with experimental data can be achieved for $\Delta = 15r_0$ and $\alpha = 1.5$. The plasma absorption coefficient distribution, given by equation (5), is a very approximate qualitative description. However, it serves well to demonstrate the possible effect of the absorption of the laser beam in the keyhole plasma on the penetration depth and show that the detailed study of plasma plume is extremely important for the creation of an adequate laser welding model.

The set of equations (1)–(5) allows us to compute the trajectory of the hump motion in the beam interaction area:

$$z \to h(t) = \int_0^t v_d(z(t), r(t))\,dt \quad (6)$$

and

$$r(t) = r_{th} + v_s t \quad (7)$$

where r_{th} (negative in our case) is the threshold position along the r-axis where the absorbed intensity of laser beam equals to I_{th}, i.e. where the drilling occurs and the keyhole wall begins propagating into the sample. Equation (6) is integrated until the absorbed beam intensity becomes lower than the threshold I_{th}. After that, integration will not result in increase of $h(t)$ since the drilling velocity becomes zero. The maximum reached value of the hump z-coordinate is the welding penetration depth, $h_w = \max(h(t))$.

Of course, the simplified approach described is applicable to simulate only the conditions when the runaway instability occurs. Otherwise, the local drilling velocity can not be assumed as parallel to the beam axis. Then a more complicated approach, which is under current development in the Sandia National Laboratory, must be used. Theoretical results of the modelling of the keyhole wall dynamics [12] show that the welding with 1–10 kW beam power, up to several hundred micrometres beam radius, and a translation speed in the range of 0.01–0.1 m s^{-1} corresponds to the conditions of the runaway instability generation. This justifies the approach proposed in [10] and further developed in this article.

3. Experiment

The laser used for this experiment was a Rofin Sinar 1200SM fast axial flow CO2 laser capable of generating 1650 W. Prior to the measurements of welding penetration depth dependencies, the focused beam geometrical parameters were characterized. Namely, the beam radius at the $1/e^2$ intensity level was measured at seven power levels from 200 to 1600 W for two different focal length focusing lenses—63.5 mm Aspheric and 127 mm Plano Convex. Laser beam characterization was performed with Prometec UFF 100 Laserscope [16]. A numerical curve fitting routine was used to determine the minimum spot size, focal plane position, and beam quality characteristics (M^2). An example of the beam characterization data is given in figure 2. The measurements show that due to beam absorption in the resonator mirrors and focusing lens, the focal position can shift by a significant value. Thus, prior beam characterization is absolutely necessary for the accurate measurements of the dependence of the welding depth on the focal plane position.

The bead-on-plate welds were made on 12.7 mm thick 304 stainless-steel and 1018 carbon steel specimens. Helium was used as a shielding gas. Welds were metallographically prepared and measured for depth, width, and area. The 12 welds per specimen were made, the specimens were sectioned in two places for penetration measurements, and the results were averaged.

4. Comparison of experimental data and simulation results

In particular, the measurements showed an important result. Namely, it was observed that the diverging beam (focus above the surface) has deeper penetration than the converging

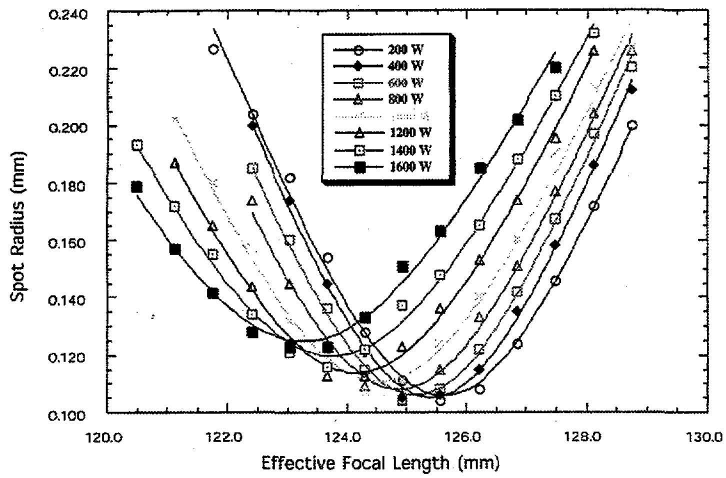

Figure 2. Beam radius at different laser power levels.

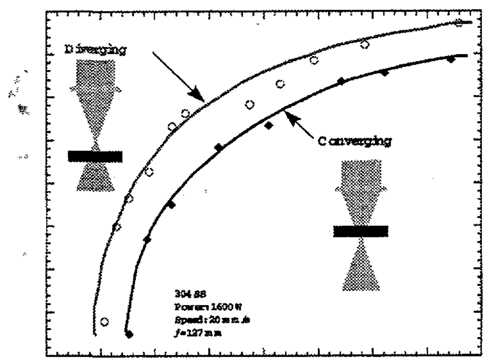

Figure 3. The effect of out of focus position on penetration.

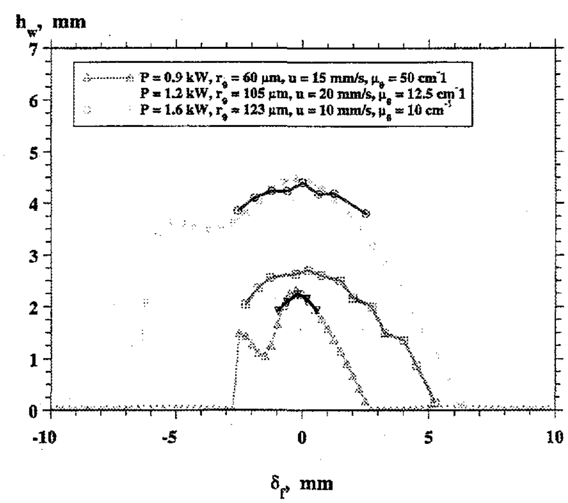

Figure 4. Comparison of measured (bold curves) and calculated dependences of welding depth, h_w, on the focus position of a laser beam δ_f.

beam (focus below the surface), provided the beam irradiance at the sample surface is the same (figure 3). This result obviously contradicts the well known belief among application engineers that the maximum penetration depth in welding is reached when the focal position of the beam lies below the sample surface. These data are also in contradiction with the recent measurements [17], which showed that the converging beam penetrates a welded specimen more deeply. Thus it appears that, depending on the processing conditions, the maximum welding depth can be obtained with either a converging or a diverging beam. The hypothesis, which we suggest and verify numerically in this work, is that the absorption in the nearsurface plasma determines the conditions which correspond to one or another case. Therefore, the contradiction between the mentioned experimental results is apparent. The mentioned data were collected under the conditions corresponding to the different values of plasma absorption coefficient and simply cannot be compared directly.

The application of the transient model, which includes absorption in the keyhole plasma, to simulate the results of the experimental measurements proved to be quite successful (figure 4). The numerical data presented in figure 4 were obtained by variation of only the maximum plasma absorption coefficient μ_0 and keeping the parameters, Δ and α, constant. Currently, the codes for the calculation of the distribution of the absorption coefficient in the keyhole plasma do not exist. Therefore to obtain the closest match of calculated dependences with the experimental data we had to select the values of μ_0, Δ, and α in the suggested distribution of the plasma absorption coefficient given by equation (5). The value of Δ effects the shape of the $h_w(\delta_f)$ dependence in the area of negative δ_f. The value of α influences the sharpness of the 'wings' of the $h_w(\delta_f)$ dependence and the values of the δ_f at which $h_w(\delta_f) = 0$. As mentioned above, the best coincidence with the experimental curves was achieved for $\Delta = 15r_0$ and $\alpha = 1.5$. These parameters were kept constant for all the numerical cases presented in this article, and only the plasma absorption coefficient, μ_0, was varied. We should mention that, possibly, to simulate

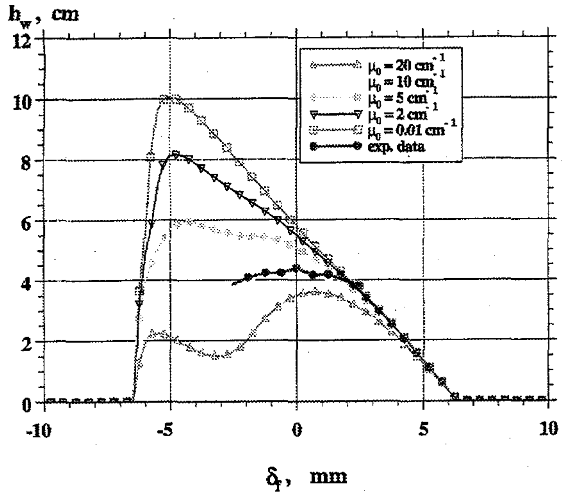

Figure 5. Dependence of the weld depth on the focus position relative to the sample surface (negative—focus inside the sample) calculated for the different plasma absorptivities μ_0, and for $P = 1.6$ kW, $r_0 = 123$ μm, $u = 1$ cm s^{-1}.

correctly the welding depth against focal position dependence under the conditions very different from the discussed in this article, some different values for Δ and α should be used. This uncertainty will be resolved only when a self-consistent evaporation–vapour gas dynamics–vapour plasma formation code is developed.

The qualitative dependence of the maximum plasma absorption coefficient on the maximum laser beam intensity is consistent with logical expectations. The plasma absorption coefficient is expected to increase with the beam intensity increase. Indeed, the values of $\mu_0 = 50$ cm^{-1}, $\mu_0 = 12.5$ cm^{-1}, and $\mu_0 = 10$ cm^{-1} gave the closest coincidence with the experimental data presented in figure 4 and obtained for the beam intensities in the focal plane of 15 MW cm^{-2}, 6.9 MW cm^{-2} and 6.7 MW cm^{-2}, correspondingly. The numerical results show that if the plasma absorption coefficient is assumed to be high then the simulation is similar to the experimental welding depth against focus position dependences (figure 4) with deeper penetration for the diverging beam when plasma absorption is higher (figure 5).

To simulate the effect of plasma on the dependence of the welding penetration depth on the focal position of the laser beam, a numerical experiment was performed. In this numerical experiment the penetration depth dependence was calculated for the different values of the maximum absorption coefficient μ_0, keeping the rest of the parameters constant. Of course, the value of the plasma absorption coefficient μ_0 depends on the beam intensity and geometrical parameters. However, in this numerical experiment we assumed that we can vary the plasma absorption coefficient independently of the beam parameters. This can correspond to a quite elaborately set real experiment when the wavelength of the laser light is varied such that the beam absorption in the plasma is different, but the rest of the interaction parameters are kept the same. Perhaps, such an experiment can be designed for at least two wavelengths corresponding to the CO_2- and Nd:YAG lasers.

The results of the numerical experiment showed that if the plasma is assumed to be weakly absorbing, the maximum penetration is achieved when the focal plane is located inside the sample (figure 5). If plasma is almost non-absorbing ($\mu_0 = 0.01$ cm^{-1}) then for a laser power of 1.6 kW, beam radius in the focal plane of 123 μm on the $1/e^2$ intensity level, and translation speed of 1 cm s^{-1}, the predicted maximum welding depth of 10 mm can be reached in steel if the focal plane is approximately 5 mm inside the sample (figure 5). The increase of maximum plasma absorption coefficient μ_0 results in a decrease of the penetration depth and a shift of the maximum in the dependence of the welding depth on the focal position towards the sample surface. When $\mu_0 = 10$ cm^{-1}, the dependence $h_w(\delta_f)$ is close to the experimentally observed results for the CO_2 laser wavelength and the function $h_w(\delta_f)$ has its maximum when focus is at the sample surface, i.e. $\delta_f = 0$. Further increase of the plasma absorption coefficient in our numerical experiment resulted in the welding depth dependence on the focal plane position with a maximum above the sample surface (figure 5 calculation data for $\mu_0 > 10$ cm^{-1}).

This result is qualitatively consistent with the observations of the experimentalists; at lower beam intensities the maximum penetration depth is reached when the focus is inside the sample and at high beam intensities the maximum of penetration is reached when the focus is at or above the sample surface [18]. Indeed, for a 3 kW CO_2 laser focused to a 200 μm beam radius with the beam divergence of a twice Gaussian beam, the intensity in the focal plane is about 2.5 MW cm^{-2} and the plasma absorption coefficient $\mu_0 = 10$ cm^{-1} gives close to the experimentally observed maximum penetration of 4.5 mm for the focus approximately 1 mm below the surface (figure 6). For a 10 kW laser with the same beam parameters, the intensity of the beam in the focal plane is approximately 7.5 MW cm^{-2}. This is a higher intensity and it is logical to assume that the plasma has a higher absorption coefficient. If, for example, $\mu_0 \sim 7$ cm^{-1} then the maximum penetration of approximately 8.5 mm is predicted for the beam focus located at approximately 1 mm above the sample surface (figure 6).

Thus, our model predicts the existence of both ranges of the interaction conditions when the converging beam penetrates the sample more deeply (keyhole plasma absorption coefficient is low) and when the diverging beam penetrates more deeply (keyhole plasma absorption coefficient is high). The contradictory experimental observations, such as shown in figure 3 and reported in [17], are not in disagreement, and in reality they represent the different pieces of a wider picture.

Two important notes must be made here. First, the plasma absorption coefficient depends on the beam intensity and not on the beam power. Therefore, qualitatively similar to the high-power case, dependence, when maximum of penetration depth is slightly above or at the sample surface, can be achieved for a low power (figure 4 for $P = 0.9$ kW, $r_0 = 60$ μm), provided the beam intensity is high ($I_0 = 15$ MW cm^{-2} in the particular case). Second, it is also reasonable to assume that the plasma absorption coefficient

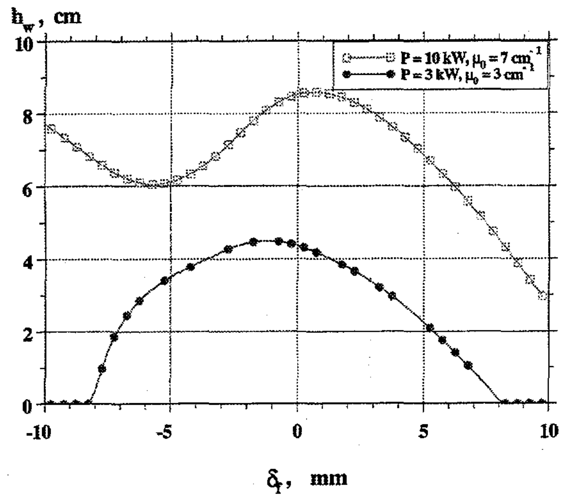

Figure 6. Calculated dependence of the weld depth on the focus position relative to the sample surface (negative—focus inside the sample) for the different laser powers and plasma absorptivities μ_0. The intensity distribution is assumed to be Gaussian with the beam divergency twice the TEM00 mode, the beam radius in focus is $r_0 = 200$ μm, and the beam translation speed $u = 2.54$ cm s^{-1}.

depends on the beam radius. The results of our calculations show that, for the same beam intensity (figure 4 $P = 0.9$ kW, $r_0 = 60$ μm and figure 6 $P = 10$ kW, $r_0 = 200$ μm), the higher value of the plasma absorption coefficient must be used for a smaller beam radius to match the experimental data ($\mu_0 = 50$ cm^{-1} and $\mu_0 \sim 7$ cm^{-1}, correspondingly). This can be explained as follows. The restriction of the lateral expansion of the plasma, as it is in the keyhole where ionized vapour escapes only through the opening, can result in a higher vapour density. Consequently, the concentration of free electrons increases, resulting in higher absorption. The keyhole transverse dimension is related to the beam radius, therefore the plasma absorption coefficient is also a function of the beam radius. The results of experimental observations confirm that the restriction of the lateral expansion of a plasma plume, indeed, results in the increase of the beam absorption in plasma [19]. This indicates that the consideration of the gas dynamics of the ionized vapour in the keyhole is very important for the creation of an adequate welding model.

5. Conclusions

The experimental measurements of the welding depth as a function of the focal plane position were performed using a low–moderate power CO_2 laser. The laser beam was carefully characterized by measuring the beam radius at different distances from the focusing lens at different laser power levels. This preliminary beam characterization allowed us to obtain accurate experimental dependences of welding depth on the beam focus position.

A transient model for the simulation of the front keyhole wall propagation into material, proposed recently [10, 11], was applied to simulate the welding penetration depth for different processing conditions. In particular, for the first time the dependence of penetration depth on focal plane position was numerically predicted. The results of the numerical experiments show that the absorption of the laser beam in the keyhole plasma plays an important role and determines the location of the beam focal position corresponding to the maximum penetration. The calculation results indicate that if the beam absorption in the keyhole plasma is low, the maximum welding depth is reached when the focal position is below the sample surface. In the case of increasing the absorption in the keyhole plasma, the position of beam focus, corresponding to the maximum penetration depth, is located above the surface. The comparison with the experimental data shows good coincidence and demonstrates large practical capabilities of this new approach.

References

[1] Andrews J G and Atthey D R 1976 *J. Phys. D: Appl. Phys.* **9** 2181–94
[2] Klemens P G 1976 *J. Appl. Phys.* **47** 2165–74
[3] Dowden J, Postacioglu N, Davis M and Kapadia P 1987 *J. Phys. D: Appl. Phys.* **20** 36–44
[4] Kaplan A 1994 *J. Phys. D: Appl. Phys.* **27** 1805–14
[5] Rosenthal D 1946 *Trans. ASME* **48** 848–66
[6] Anisimov S I and Khokhlov V A 1995 *Intabilities in Laser–Matter Interaction* (Boca Raton: CRC Press)
[7] Semak V and Matsunawa A 1997 *J. Phys. D: Appl. Phys.* **30** 2541–52
[8] Afanasiev Yu V and Krokhin O N 1967 *Sov. Phys. JETP* **25** 639
[9] Semak V V, Hopkins J A, McCay M H and McCay T D 1994 *Proc. ICALEO'94* pp 830–7
[10] Fabbro R and Poueyo-Verwaerde A 1995 *Proc. ICALEO'95* pp 979–88
[11] Semak V V, Hopkins J A, McCay M H and McCay T D 1994 *Proc. ICALEO'94* pp 641–50
[12] Matsunawa A and Semak V 1997 *J. Phys. D: Appl. Phys.* **30** 798–809
[13] Semak V and Matsunawa A 1997 *J. Phys. D: Appl. Phys.* **30** 2541–52
[14] Semak V V, Bragg W D, Damkroger B and Kempka S 1999 *J. Phys. D: Appl. Phys.* **32** L61–4
[15] Essein M and Fuerschbach P 1996 *Welding J./Welding Res. Suppl.* **75** 47-s–54-s
[16] Steele R J, Fuerschbach P W and MacCallum D O 1997 *Proc. ICALEO'97* pp 167–76
[17] Tsukamoto S, Hiraoka K, Asai Y, Irie H and Oguma M 1998 *Proc. 5th Int. Conf. on Trends in Welding Research* to be published
[18] Duhamel R Convergent energy private communication with V V Semak
[19] Semak V V 1991 Interaction of microsecond laser pulses with a target in the presence of ambient gas *PhD Thesis* Moscow Institute of Physics and Technology, Moscow (in Russian)

Sandia is a multiprogram laboratory operated by Sandia Corporation, a Lockheed Martin Company, for the United States Department of Energy under contract DE-AC04-94AL85000.